SCIENTIFIC REPORTS

OPEN

SUBJECT AREAS:
MOLECULAR NEUROSCIENCE
GENE EXPRESSION
BRAIN
GENE REGULATION

Received
24 August 2012

Accepted
10 October 2012

Published
7 November 2012

Correspondence and requests for materials should be addressed to M.K. (kake@m.u-tokyo.ac.jp)

* Current address: Department of Integrative Physiology, Gunma University Graduate School of Medicine, Gunma 371-8511, Japan.

Fluorescence laser microdissection reveals a distinct pattern of gene activation in the mouse hippocampal region

Wataru Yoshioka[1], Nozomi Endo[1], Akie Kurashige[1], Asahi Haijima[1]*, Toshihiro Endo[1], Toshiyuki Shibata[1,3], Ryutaro Nishiyama[2], Masaki Kakeyama[1] & Chiharu Tohyama[1]

[1]Laboratory of Environmental Health Sciences, Center for Disease Biology and Integrative Medicine, Graduate School of Medicine, The University of Tokyo, Tokyo 113-0033, Japan, [2]Research/Clinical/Industrial Division, Leica Microsystems K.K., Tokyo 108-0072, Japan, [3]Department of Human Ecology, Graduate School of Medicine, The University of Tokyo, Tokyo 113-0033, Japan.

A histoanatomical context is imperative in an analysis of gene expression in a cell in a tissue to elucidate physiological function of the cell. In this study, we made technical advances in fluorescence laser microdissection (LMD) in combination with the absolute quantification of small amounts of mRNAs from a region of interest (ROI) in fluorescence-labeled tissue sections. We demonstrate that our fluorescence LMD-RTqPCR method has three orders of dynamic range, with the lower limit of ROI-size corresponding to a single cell. The absolute quantification of the expression levels of the immediate early genes in an ROI equivalent to a few hundred neurons in the hippocampus revealed that mice transferred from their home cage to a novel environment have distinct activation profiles in the hippocampal regions (CA1, CA3, and DG) and that the gene expression pattern in CA1, but not in the other regions, follows a power law distribution.

A multicellular organism consists of various kinds of tissue composed of heterogeneous cell types. To clarify the physiological and pathological roles of a cell under a given condition, information on the abundance of gene products as well as the localization of the cell within the tissue is extremely important because the regulation of gene expression in a particular cell is not only influenced by the type of cell but is also regulated by signals from the surrounding environment[1]. In conventional histological analyses, such as *in situ* hybridization (ISH), the morphology is preserved, but, the estimated expression level is of a semi-quantitative nature. Thus, we anticipate that a histological method in combination with a sensitive and quantitative mRNA detection method, such as reverse transcription-quantitative polymerase chain reaction (RTqPCR), will enable to determine the gene expression level in a specific cell or region of a tissue, and provide useful information on the unique function of a cell or region.

To obtain a specific type of cell from a given tissue for gene expression analysis, a number of methods, such as tissue resection, punch-out, fluorescence-activated cell sorting (FACS), and laser microdissection (LMD), have been available. Among these methods, FACS has an advantage over the other methods in terms of isolating and enriching for a particular cell type[2]. However, the information obtained from FACS analysis does not have histological context of the harvested samples, which is similar to *in vitro* methods using cultured cells. On the other hand, LMD is superior to the other methods in terms of identifying a distinct area as the region of interest (ROI) and collecting it under microscopy. In the LMD system, an ROI is arbitrarily shaped and sized, which can be as small as the size of a single cell[3], and theoretically, could be downsized to the sub-cellular structures, such as the dendrite, spine, and organelle. Despite the superiority of the LMD method to other methods, it has not been used as a routine method probably due to the following reasons: (1) RNA degradation during histological processing, (2) requirement of sophisticated techniques to quantify small amounts of RNAs obtained from small tissue sample, and (3) necessity of a sufficient contrast of signal and noise ratio for the staining to clearly visualize the border of a small ROI from the background. In this study, we report a technological advance in fluorescence LMD-RTqPCR method that is capable of detecting ROIs identified by fluorescence probe, retaining RNAs during the histological process, and determining the absolute ultra-microquantity of target RNAs without pre-amplification. This method enables to compare the RNA abundance of a particular gene in different ROIs, or that of a variety of genes in a particular ROI. Using this method, we quantified the abundance of immediate early genes

(IEGs) in ROIs from the mouse brain, and found distinct profiles of gene activation in the hippocampal regions (CA1, CA3, and DG) of mice, placed in a novel environment.

Results

Validity of ultra-microquantification of RNA. The LMD system used in this study emits pulse laser beams to cut along the outer border of the ROI under a microscope to collect it with a minimal degree of damage in the ROI (Fig. 1a). Utilizing the force of gravity, this method allows the laser-exposed specimen to fall off directly into a sampling-microtube placed beneath the slide, which allows the collected specimen to maintain the morphology of the ROI (Supplementary Fig. 1). To reap the full advantage of the LMD system for detecting fluorescent-labeled specific cells of research interest, we have recently developed a fluoropolymer membrane slide that minimizes background fluorescence (Supplementary Fig. 2c vs. 2a; 2d vs. 2b), which increases the efficiency of identifying fluorescence-labeled single cells in tissue sections, compared with a polyethylene polyphthalate slide (Supplementary Fig. 2a, c).

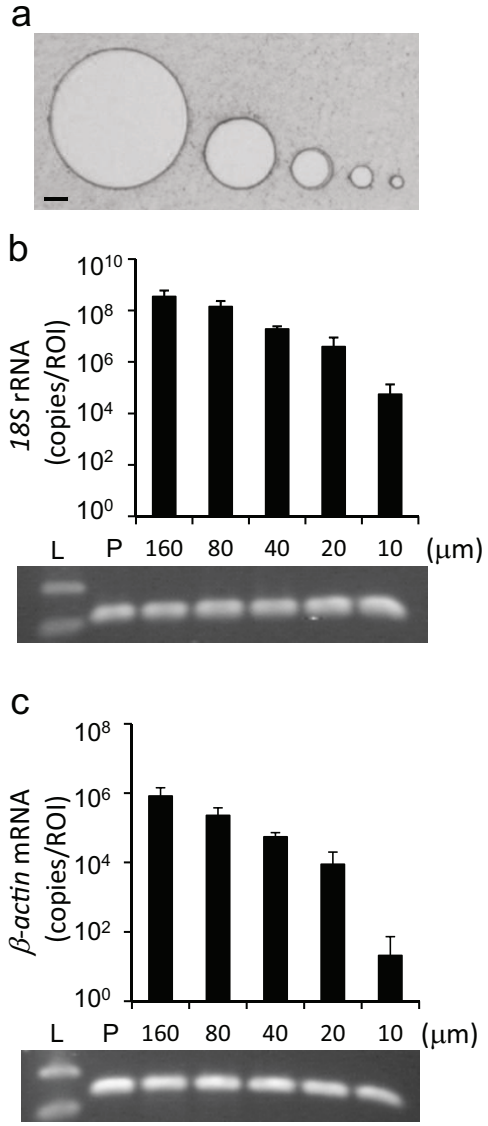

Figure 1 | Quantification of RNAs in ROIs of various sizes. (a) Representative image of an unstained brain section (8 μm) after obtaining ROIs, having diameters of 160, 80, 40, 20, and 10 μm, by LMD. Scale bar = 20 μm. The area inside the laser-burned ring-shaped 'scar' was collected for RNA analysis. (b, c) The obtained ROIs, with diameters ranging from 160 - 10 μm, were lysed to produce cDNA, and the amounts of *18S* rRNA and *β-actin* mRNA were quantified by RTqPCR using specific primers (Supplementary Table 1). The result from gel electrophoresis is presented to show the size of PCR products after amplification to the saturation phase of RTqPCR. 'L' and 'P' indicate the DNA ladder as size markers and the positive control derived from a mouse brain extracted and amplified using standard methods, respectively. Lanes in the gel electrophoresis correspond to the bars above.

To accurately analyze the gene expression of ultra-microquantities of mRNA obtained from laser-microdissected samples, three alterations were made to the conventional RNA preparation protocol. First, 'carrier RNA' was added to the microtubes in which the cDNA is synthesized from the mRNA obtained from the ROI. Because plastic microtubes have a tendency to adsorb nucleic acids, as shown by an incubation experiment using 10^6 copies μl^{-1} of *β-actin* DNA fragments (Supplementary Fig. 3a), 'carrier RNA' was added to minimize the loss of mRNA obtained from the extremely small amounts from the tissue sample. The 'carrier RNA' was designed to have a similar structure to chum RNA[4] with no specific tertiary structure, which was predicted by the m-fold program[5], and no sequence homology to any mouse cDNA, which was confirmed by BLAST. The efficaciousness of the 'carrier RNA' on preventing the adsorption of the nucleic acid sample by the plastic microtubes is clearly shown. The *β-actin* DNA fragments recovered within 6 days was significantly less when the nucleic acid sample was incubated without 'carrier RNA' (Supplementary Fig. 3a). In contrast, incubating the *β-actin* DNA fragments with the 'carrier RNA' was found to maintain the quantity of the sample at approximately the same level as the initial quantity for at least four weeks (Supplementary Fig. 3b). Second, our method requires neither purification nor quantification of total RNA, and utilizes a single microtube, which minimizes the loss of the RNA sample during this process. Third, we considerably reduced the time required for histological staining, and treating the ROI with proteinase K to release the RNA from the fixed tissue, and optimized and verified the RNA detection method. Such alterations were found to be effective to preserve the fluorescence proteins in the tissue samples that were perfused and fixed with a 4% paraformaldehyde solution.

To verify the sensitivity and precision of the LMD-RTqPCR method, samples from the ROIs (8 μm in thickness) with diameters ranging from 160 to 10 μm (Fig. 1a) were prepared and analyzed for *18S* rRNA and *β-actin* mRNA content. The results show a linear decrease in the amount of *18S* rRNA and *β-actin* mRNA that was proportional to the diameter of the samples to approximately 10 μm (Fig. 1b, c). Furthermore, the amount of *18S* rRNA and *β-actin* mRNA was also proportional to each other in samples in different size (Supplementary Fig. 4). These results indicate that the amount of *18S* rRNA and *β-actin* mRNA in samples could be used to normalize the data according to the size of the ROI. Thus, the RNA detection method used in this study is thought to be sufficiently sensitive and precise for the quantification of gene expression in samples obtained from an ROI of a single cell size.

To determine if our fluorescence LMD-RTqPCR method is sensitive enough to analyze the gene expression in a cell-sized ROI, we used the NeuroTrace, a green fluorescnent Nissl staining, to visualize neurons, and *in utero* electroporation (IUE) technique[6] to visualize a specific neuron population in the mouse neocortex. In the IUE, the *mCherry* gene that encodes a red fluorescence protein[7] was transferred by *in utero* electroporation into the neurons in the upper cortical layer of fetal mice (Fig. 2a). The ROI in this case corresponded to a single neuron, which was labeled and identified by NeuroTrace and mCherry. Ten Nissl-positive cell-sized ROIs with or without mCherry fluorescence were collected in microtubes and compared in terms of their gene expression levels (Fig. 2b). The abundance of *β-actin* mRNA, a housekeeping gene, and *Map2* mRNA, a neuron-specific marker, in the mCherry-positive and

mCherry-negative neurons was found to be equivalent. Furthermore, *mCherry* mRNA was only detected in the mCherry-positive cells (Fig. 2b), indicating that cross-contamination during the LMD process was negligible.

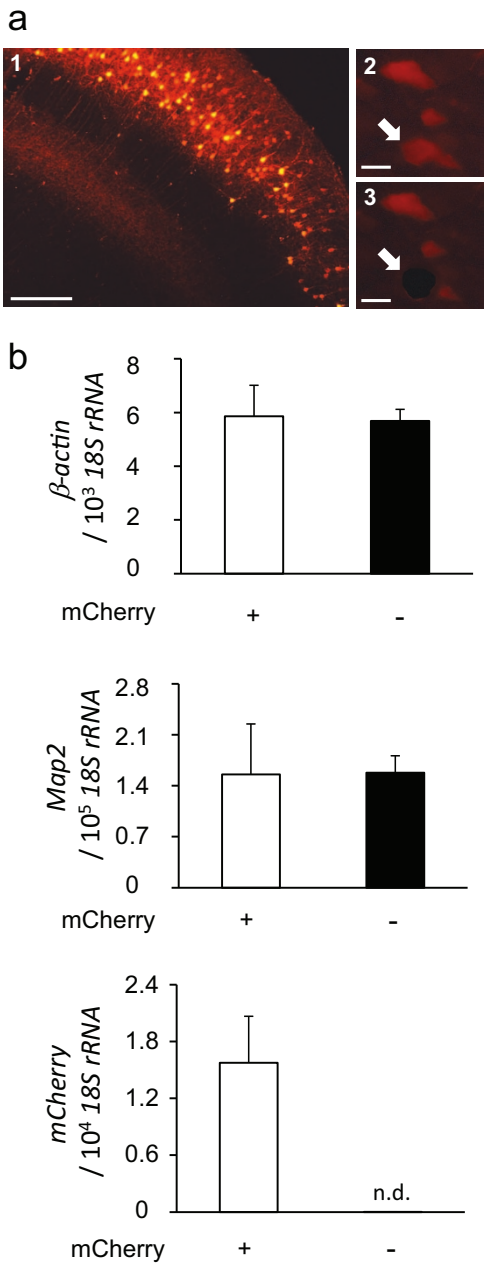

Figure 2 | Quantification of mRNAs in cell-sized ROIs from mouse cortical sections. Newborn neurons at embryonic day 15 were transfected with the red fluorescence gene *mCherry* and migrated into the upper layers of the neocortex. The brain section (14 μm) was stained by green fluorescent Nissl immunohistochemistry. (a1) Photomicrograph of a representative mouse brain cortical section labeled with mCherry (red). The mCherry signal is used as a fluorescent marker for neurons in which the gene was transfected by *in utero* electroporation. (a2, 3) Magnified photomicrographs of A1 before and after dissection by LMD. Scale bars = 200 μm (a1) and 5 μm (a2, a3). (b) Quantification of mRNAs in the ROIs corresponding to mCherry-positive and mCherry-negative neurons. mCherry-negative cells were identified as neuron by the fluorescent Nissl signal. Please see Methods for details on the *in utero* electroporation of *mCherry* in mice. "n. d." indicates that the amounts were too low to be detected.

Quantification of hippocampal region-dependent gene expression. We used the fluorescence LMD-RTqPCR method to quantify the gene expression levels in specific regions of the mouse hippocampus, the dentate gyrus (DG) and cornu ammonis 3 (CA3). Although the ISH data from the Allen Brain Atlas project indicates that several genes are expressed in a "region-enriched" manner[8], the extent of enrichment for a particular gene has been unknown. In the present study, we stained neurons in hippocampal sections with NeuroTrace and laser-microdissected portions of neuronal cell layers of the DG and CA3 (Fig. 3a). The size of ROIs that were collected for this experiment was 20,000–30,000 $\mu m^2 \times 14$ μm, and these ROIs were estimated to have two to three hundred neurons. The gene expression levels were compared after normalization to *18S* rRNA so that an accurate comparison between ROIs of different sizes could be made. The abundance of *calb1* and *pcp4* mRNA was 84 and 19 times greater, respectively, in the DG than

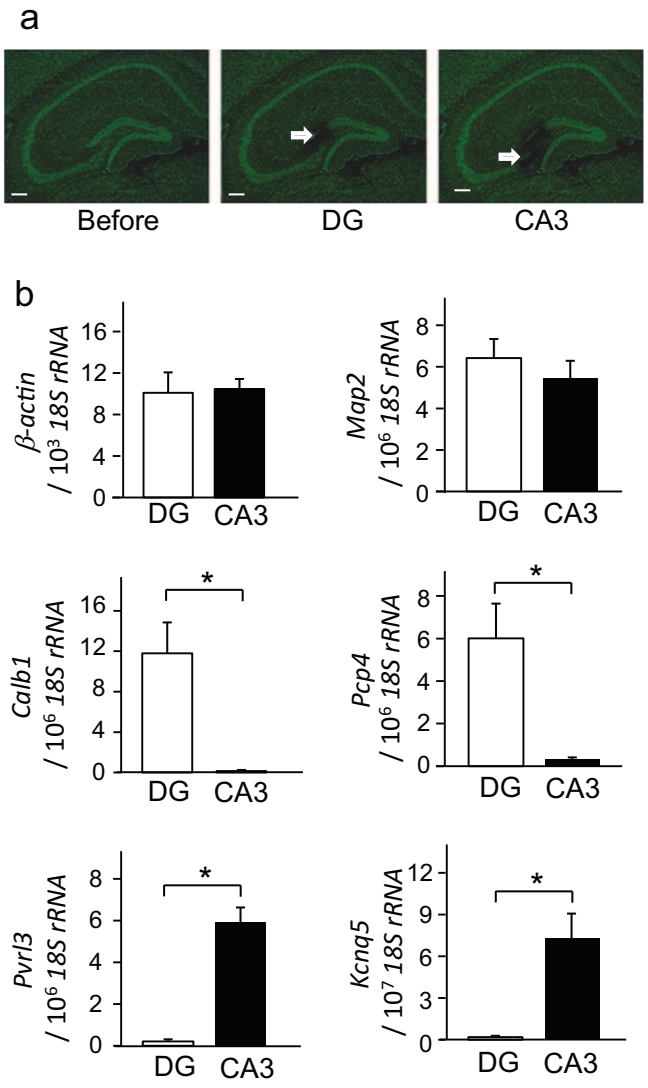

Figure 3 | Quantification of mRNAs in the ROIs from specific subregions of the mouse hippocampal section. Neurons were immunohistochemically labeled by NeuroTrace, a green fluorescent Nissl antibody, and each portion of hippocampal region was successfully and precisely dissected as ROIs. (a) Brain sections (14 μm) before dissection (left), after dissection of a portion of the DG (middle), and the CA3 (right). Scale bars = 100 μm. (b) Abundance of RNAs in the ROIs in the DG and CA3 subregions are shown. *Significantly different according to Welch's *t*-test at $p < 0.05$.

the CA3, and the abundance of *pvrl3* and *kcnq5* mRNA was 28 and 38 times greater, respectively, in the CA3 than the DG (Fig. 3b). Such quantitative comparisons for abundance of a particular gene between the ROIs were made possible by absolute determination using a standard curve for each gene. Notably, *β-actin* mRNA expression levels in the DG and CA3 appeared to be equivalent, which confirms the effectiveness of normalizing samples using 18S rRNA. In addition, *Map2,* a marker gene for neurons, was expressed at approximately equivalent levels in the DG and CA3, indicating that there is a comparable abundance of neurons in these regions. Altogether, these results show that the DG and CA3 have substantially different gene expression patterns, and our findings are the first to report the exact degree of "enriched" expression of a particular gene.

Distinct gene expression profiles of immediate early genes activated by a novel environment. Next, we applied our fluorescence LMD-RTqPCR method to a quantitative analysis of immediate early genes (IEGs) induced in the hippocampus of mice. It has been established that hippocampal IEGs are upregulated when mice are placed to a novel environment[9]. It is still unknown, however, how much these IEGs are upregulated, or in which regions of the hippocampus these changes occur. To obtain such quantitative information, mice housed in their home cage (HC) were individually transferred to a novel environment (NE), and the abundance of nine IEG mRNAs in the CA1, CA3 and DG regions was determined (Fig. 4). As to the average basal abundance of the IEGs from the HC group, the highest and lowest expression levels were observed in *BDNF* (20.4 copies/10^6 copies *18S* rRNA), and *Egr2* (0.039 copies/10^6 copies *18S* rRNA), respectively. Mice that were placed in the novel environment, NE group, were found to have significantly altered abundance of some of the IEG mRNAs. When a fold increase was calculated by dividing the average abundance in the NE group by the one in the HC group, for example, the expression of *Egr2*, *cFos* and *cJun* in the CA1 increased 19.9, 9.25 and 6.58, respectively. This quantitative analysis was made possible

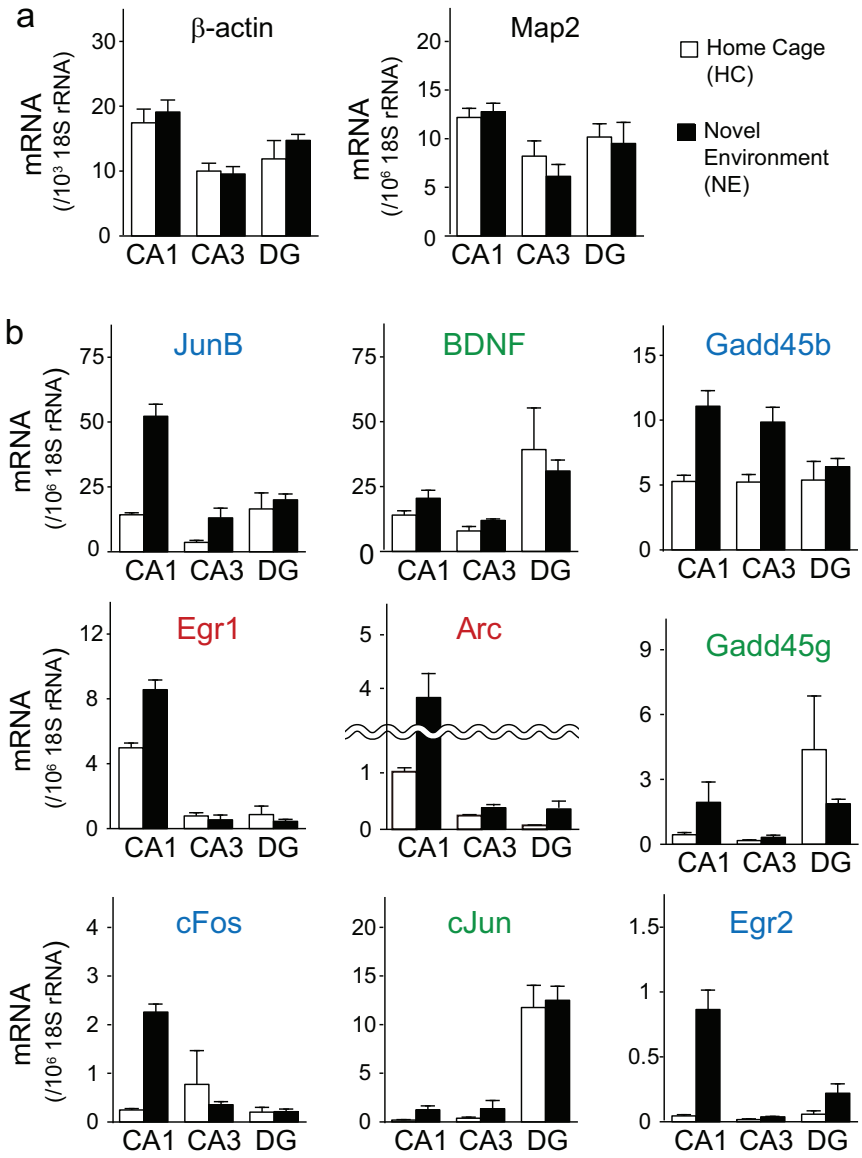

Figure 4 | Quantification of IEG mRNAs in the ROIs from specific regions of mouse hippocampal sections. Mice were exposed to 10 minutes of stimulus by being placed in a novel environment (NE group, n= 4) or kept in a home cage (HC group, n= 4). Brain sections (10 μm) were dissected by LMD to collect a portion of the CA1, CA3 and DG of the hippocampus. (a) A house keeping gene, *β-actin*, and a neuron marker gene, *Map2*. (b) Immediate early genes (IEGs).

because the number of copies of each IEG in a particular ROI was determined. It was also revealed that the hippocampal regions studied as ROIs have their own distinct expression profiles of IEGs (Fig. 4b): *cJun* mRNA was more abundant in the DG (11.7 copies/10^6 copies *18S* rRNA) than in the CA1 (0.19 copies/10^6 copies *18S* rRNA) and CA3 (0.38 copies/10^6 copies *18S* rRNA), whereas *Egr1* mRNA was more abundant in the CA1 (4.98 copies/10^6 copies *18S* rRNA) than in the CA3 (0.76 copies/10^6 copies *18S* rRNA) and DG (0.86 copies/10^6 copies *18S* rRNA). *β-actin* and *Map2* were expressed at similar levels in the CA1 and DG and at slightly lower levels in the CA3 (Fig. 4a). The number of IEGs activated by placing mice in a novel environment differed considerably depending on the region (Fig. 4b). In the CA1, six (*Arc, cFos, Egr1, Egr2, Gadd45b* and *JunB*) out of nine IEGs were upregulated by this stimulation, whereas only two (*JunB* and *Gadd45b)* and none were upregulated in the CA3 and DG, respectively.

When the mRNA abundance for each IEG was subjected to z-score transformation, region-specific gene expression patterns were clearly revealed (Fig. 5a). In the CA1, the difference in abundance of IEGs between the HC and NE groups was found to be proportional to the abundance of mRNAs in the HC. On the other hand, the ratio of mRNA abundance in the HC group over the NE group was found to be inversely proportional to the abundance of mRNA in the HC (Fig. 5a). We plotted the average basal abundance of each IEG on the x-axis and the fold increase in gene expression, i.e., a ratio of the average abundance in the NE group over the HC group, of the same IEG on the y-axis (Fig. 5b, left) and found that all of the IEG data do not show any correlations, suggesting that the expression of the IEGs appears to be independent from each other. When the data on the scatter graph were categorized by hippocampal region (Fig. 5b, right), however, the fold increase in gene expression of IEGs in the CA1 appears to conform to a power law, which is expressed as [fold increase] = 4.44 × [basal level]^(−0.36), with r^2 = 0.89, p = 0.00014. This observation may reflect the reactivity of the CA1 to the novel-environmental stimulus.

Discussion

In this study, we made a technological advance in a fluorescence LMD-RTqPCR method that is sufficiently sensitive to quantify small amounts of mRNA in ROIs isolated from tissue sections under

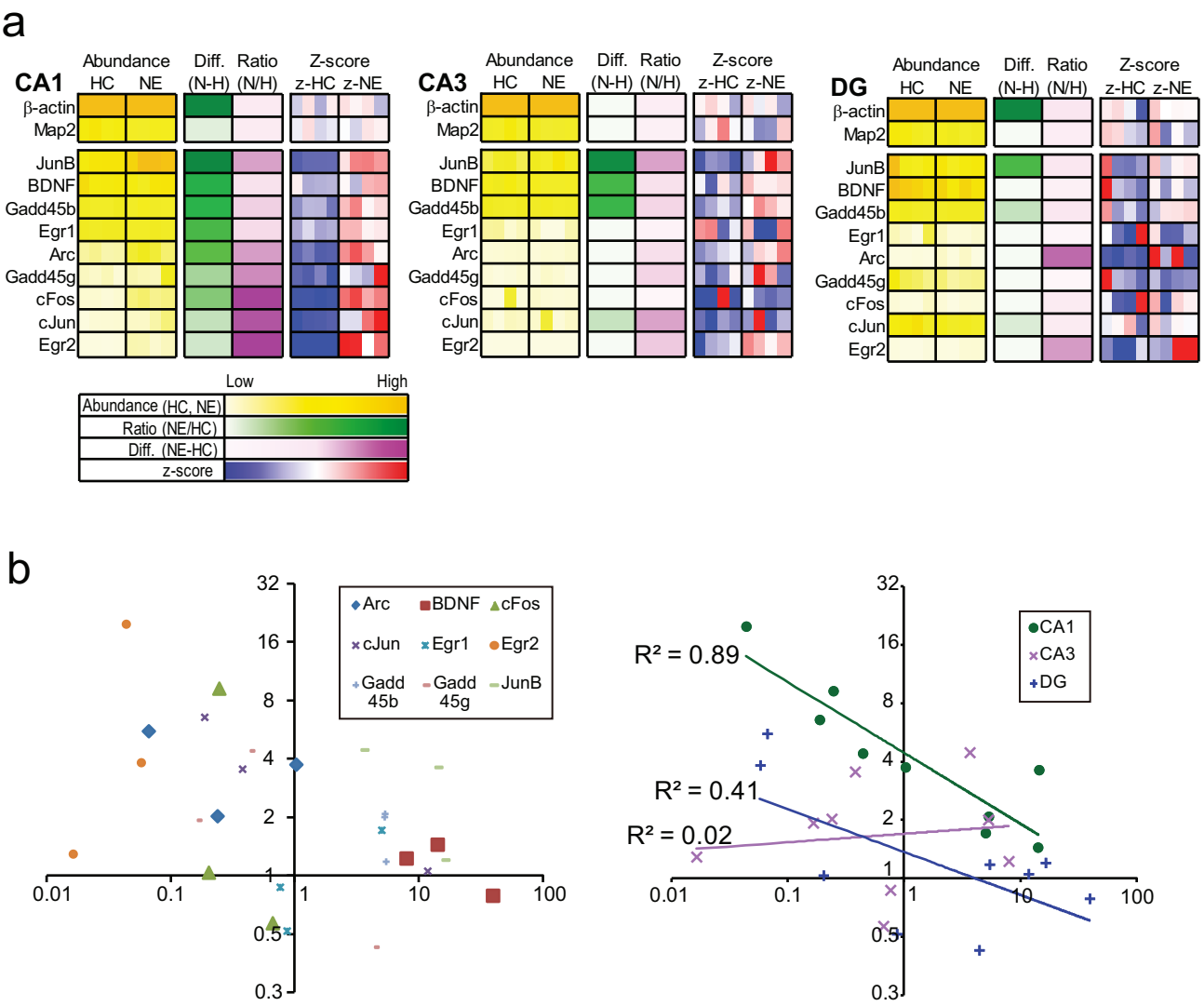

Figure 5 | (a) Gene expression modes of IEGs, that includes abundance, differences in abundance between the NE and HC groups, ratios of abundance between the two groups, and standardized expression levels (z-scores), in the CA1 (left), CA3 (middle) and DG (right). (b) A scatter plot, with the average basal abundance of each IEG on the x-axis and the average fold increase in gene expression (expressed as the ratio of the abundance in the NE group over the HC group) of the same IEG on the y-axis. In the left graph, each kind of the IEGs in CA1, CA3 and DG is shown by using the same symbol. In the right graph, IEGs are grouped on the basis of either of the CA1, CA3 and DG regions, and a significant correlation was found in the CA1.

fluorescence microscopy. This method has the following three unique features. First, it has a great advantage over previously reported methods[10–12] in terms of the size of the ROI. Our fluorescence LMD-RTqPCR method can quantify the mRNA from a single-cell sized ROI, as demonstrated by our results from an ROI having a diameter of 10 μm and our results from *mCherry*-transfected cortical neurons. Moreover, our fluorescence LMD-RTqPCR method has three orders of dynamic range, with the lower limit of ROI-size corresponding to a single cell.

Second, a fluorescence-labeled cell can be easily detected by the fluorescence LMD system because of our recently developed a new type of fluoropolymer membrane slide that minimizes background fluorescence. To confirm the applicability of this membrane slide, a specific neuronal population was labeled with the fluorescence gene mCherry by *in utero* electroporation[6,13], and neurons were stained with NeuroTrace. We found that this membrane slide is useful for isolating a cell population identified by mCherry-fluorescence from the background fluorescence, and demonstrated that our fluorescence LMD-RTqPCR method can analyze the gene expression in specific newborn-neurons in the brain at specific stages of brain development. There are bioresource depositories that contain over 2,000 strains of mice that express fluorescence genes in the database of the International Mouse Strain Resource[14]. Thus, in future studies, these mouse strains can be appropriate candidates for the application of the fluorescence LMD-RTqPCR method.

Third, gene expression levels in ROIs of different sizes can be quantitatively compared with each other after they are normalized using an internal control gene. On the other hand, in conventional histological analyses, such as ISH and IHC, the expression level of a target molecule in an ROI has been sem-quantified as the number of positive cells. This type of analysis often leads to ambiguous interpretations because cells from different regions of a particular tissue may differ in size, such as pyramidal neurons and granular neurons in the CA and DG, respectively. In the present fluorescence LMD-RTqPCR method, a number of genes can be used to normalize samples: the volume of ROI was normalized using *18S* rRNA. *MAP2* and *mCherry* can be used to normalize the expression level of target genes per neurons in general and per specific neurons, respectively. A number of other marker genes, such as *β-actin*, can also be used for normalization. Such a large number of genes that can be used to normalize samples give the fluorescence LMD-RTqPCR method great flexibility in its applicability.

The hippocampus plays a crucial role in higher brain functions, including learning and memory, and it is one of the most studied areas in the brain. The mouse hippocampus consists of the CA1, CA2, CA3, and DG region[15]. Based on the 'Allen Brain Atlas' project, an anatomically comprehensive genome-wide survey of 21,000 gene expression patterns in the adult mouse brain using ISH, several genes were identified as being highly expressed in a regionally enriched manner in the hippocampus[8]. In our study, the fluorescence LMD-RTqPCR method revealed that *calb1* and *pcp4* mRNAs are expressed in quantities more than ten times greater in the DG than in the CA3, and *pvrl3* and *kcnq5* mRNAs are expressed in quantities more than 20 times greater in the CA3 than in the DG. This dramatic difference in gene expression between the DG and CA3 suggests that they have distinct functions even though they reside in close proximity to each other. In sum, DG-enriched genes were detected in the CA3, albeit at low levels, and that CA3-enriched genes were detected in the DG, which demonstrates that the expression profiles of these regions include larger quantities of their "own-region-enriched" genes and smaller quantities of "other-region-enriched" genes. The implication of this finding is that the cell samples collected by FACS using "region-enriched" genes as a marker may result in the inclusion of a heterogeneous population that consists of cells from other regions. Conditional knock-out technology using a "region-enriched" gene is likely to have a similar problem. In contrast, the LMD system has advantages over these methods because it is able to isolate the targeted ROI with the histological context.

Application of the present fluorescence LMD-RTqPCR method to gene expression analysis of IEGs demonstrated that the CA1 region, but not the CA3 or DG of the hippocampus, is strongly activated by the stimulation of a novel environment in mice. The IEG fold increase in the CA1 was on average 5.85, whereas the fold increase in the CA3 and DG were 2.11 and 1.74, respectively. While the abundance of IEGs in the CA1 region has been reported in semi-quantitative terms[16–18], our study is the first to report the quantitative analysis of mRNA abundance in such a small area. We predict that this quantitative approach combined with fluorescent laser microdissection microscopy will reveal the distinct activation profile of IEGs.

In the CA1 region, the fold increase in the expression levels of IEGs compared with the basal expression level was found to follow a power law distribution ([fold increase] = 4.44 × [basal level]^(−0.36), with $r^2 = 0.89$, $p = 0.00014$). The IEGs analyzed in this study, such as *cFos, cJun* and *JunB*[19], *Egr1* and *Egr2*[20], and *BDNF*[21] are a member of the AP-1 family, Egr family, and neurotrophin family, respectively. *Gadd45b* and *Gadd45g* code for stress sensor proteins[22], and *Arc* is a synaptic activity responsive gene[23]. The fact that such a wide variety of genes conform to a power law distribution could be indicative of a fundamental mechanism of gene expression in response to a stimulus, and this relationship has the potential to be used as an activation indicator in a brain region because it was observed in the CA1, where most of IEGs analyzed were upregulated. Furthermore, studies on IEGs that do not follow the power law distribution may reveal specific roles of particular genes. Power law distributions have been found in many phenomena, such as neuronal avalanches in cortical networks[24] and the distribution of genes expressed at various levels[25]. Our results are thought to be another example of power law distribution.

In conclusion, the present fluorescence LMD-RTqPCR method we have developed can be used to determine the absolute amount of mRNAs in a small tissue sample that is labeled with a fluorescent probe and identifiable under microscopy. Using this method, we found that IEGs are activated in the CA1 following a power law distribution in mice placed in a novel environment. Use of this method in future studies may lead to the discovery of novel phenomena and deepen our understanding on the physiological significance of gene expression in ROIs.

Methods

Animals and tissue preparation. C57BL/6J mice were purchased from CLEA Japan, Inc. and kept in an animal room at a temperature of 23 ± 1°C, a humidity of 50 ± 10%, and on a 12/12 h light–dark cycle (lights on at 8:00). Laboratory rodent chow (Labo MR Stock, Nosan) and distilled water were provided *ad libitum*. The experimental protocols of this study were approved by the Animal Care and Use Committee of the Graduate School of Medicine, The University of Tokyo.

Mice were deeply anesthetized with pentobarbital sodium (50 mg kg^{-1} body weight i.p, Dainippon Sumitomo Pharma) and dissected without fixation (Fig. 1) or perfused transcardially with 4.0% paraformaldehyde in 0.1 M phosphate-buffered saline (PBS; pH 7.4). The brains were removed, postfixed in the same fixative solution overnight, and then immersed in a series of 0.1 M PBS solutions with increased sucrose concentrations (5.0% sucrose for 5 h, 10.0% and 20.0% sucrose overnight). Subsequently, the brain tissue was embedded in OCT compound and frozen in liquid nitrogen. Coronal sections (8–14 μm) were cut using a cryostat (CM3050, Leica Microsystems) at −20°C and mounted on two kinds of slides: polyethylene naphthalate slides (Leica Cat. No. 11505189) that have been routinely used and RNase-free metal-framed fluoropolymer membrane slides (Leica Cat. No. 11600250) that have been recently developed in our project. The sections were dried at room temperature overnight.

Fluorescent labeling. To visualize neuronal cells, fluorescent Nissl staining was performed. Tissue sections were incubated in 50-fold diluted NeuroTrace 500/525 (Molecular Probes, Eugene) at room temperature for 1 min and washed twice in 0.1 M phosphate buffer for 10 s. The sections were immediately air dried using a blower.

To transfect a specific cell with the *mCherry* gene, *in utero* electroporation was conducted as previously described[6,13]. Briefly, pregnant C57BL/6J mice were deeply

anesthetized with pentobarbital sodium (35 mg kg^{-1} body weight, i.p.) on gestational day 15. Then, the uterine horns were exposed and approximately 1 mL of pCAG-mCherry solution (a kind gift from Dr. M. Matsuzaki at the National Institute for Physiological Sciences, Okazaki, Japan) was injected into the lateral ventricle of fetal brains. Electronic pulses (35 V) were applied four times at intervals of 950 ms with an electroporater (CUY21SC; Nepa Gene). The uterine horns were returned to the abdominal cavity to allow the embryos to continue their normal perinatal development until they were sacrificed on postnatal day 30.

IEGs activation by novel environment. Adult male C57BL/6J mice were kept in a group consisting of 4–6 animals and acclimated in isolated home cages for 4 days just prior to the experiment. The novel environment consisted of a square open field box (50 (w) × 50 (l) × 40 (h) cm^3). Each mouse was placed in the center of the box, allowed to move freely for 10 minutes, and then placed back in the home cage for 30 minutes (NE group, n=4) before collecting their brain as described in 'Animals and Tissue Preparation'. Control mice were kept in home cages (HC group, n=4).

Laser microdissection and RNA preparation. Specific cells or regions were laser-microdissected using the LMD7000 (Leica Microsystems) and collected into the cap of a 0.2 ml microtube (BIO-BIK BT-02LC, Ina-Optika). At every collection, the presence of the laser-microdissected tissue sample in the cap of the microtube was confirmed by LMD microscopy. The laser-microdissected tissue samples were spun down to the bottom of microtubes by centrifugation at 15,000 x *g* for 1 min. The precipitate was dissolved in 2.0 µl of lysis buffer from the CellAmp Direct RNA Prep Kit (Takara), containing proteinase K (0.3 U, Takara) and 'carrier RNA' (10 ng, described below), and lysed completely by tapping 20 times. The samples were subsequently sonicated for 1 min and incubated in a water bath at 75°C for 5 min to inactivate the proteinase K. DNA in the lysate was digested by adding 0.5 µl of DNase I (0.05 U, Takara) and incubating at 37°C for 5 min., and then added with 2.5 µl of EasyDilution (Takara) and 2.0 µl of water and incubated at 75°C for 5 min to inactivate the DNase. The solution containing RNAs was reverse-transcribed using PrimeScript (Takara) with both oligo-dT20 and random N_6 primers according to the manufacturer's instructions. The 'carrier RNA' was designed not to have a specific tertiary structure, which was predicted by the m-fold program[5], or sequence homology to any mouse cDNA, which was confirmed by BLAST. It was *in vitro* transcribed using T7 RNA polymerase (Toyobo) and had the sequence 5′-GGACACAAGACAACAUAAAAAAAAAAAAAAAAAAAAAAAAA-3′.

RNA quantification. The quantitative detection of cDNAs was performed by SYBR Green I-based real-time PCR using a Light Cycler instrument (Roche Molecular Biochemicals) and Thunderbird qPCR mix (Toyobo). Primers for each gene (Table S1) were designed based on respective sequences using the Primer3 program[26]. Negative controls for qPCR were analyzed concomitantly to confirm that the samples were not cross-contaminated. The expression levels of RNAs (mRNAs and rRNA) are presented as copy number, which was calculated using standard curves and Light Cycler analysis software (Roche Molecular Biochemicals).

Data analysis. Data are expressed as mean ± SEM. *P*-values below 0.05 were considered to be statistically significant using Welch's *t*-test. In the experiment of activation of IEGs by the novel-environment stimulus, the average mRNA abundance of each IEG was used to derive the fold increase in gene expression of IEGs by the following formula: [the average mRNA abundance of the NE group (activated expression level)] / [the average mRNA abundance of the HC group (basal expression level)]. The regression analysis followed by analysis of variance was performed to determine the correlation between the basal expression levels and induction levels in each IEG, and/or in each brain region. The z-score for expression level of an IEG in a specimen from a region was calculated by subtracting the average copy number of specimens in the region from the copy number of the specimen, and dividing the result by the SD for the specimens in that region.

1. Shaw, K. Environmental Cues Like Hypoxia Can Trigger Gene Expression and Cancer Development. *Nature Education* **1** (2008).
2. Kalisky, T. & Quake, S. R. Single-cell genomics. *Nat Methods* **8**, 311–314 (2011).
3. Sun, H. *et al.* Laser microdissection and pressure catapulting of single human motor neurons for RNA editing analysis. *Methods Mol Biol* **718**, 75–87 (2011).
4. Tougan, T., Okuzaki, D. & Nojima, H. Chum-RNA allows preparation of a high-quality cDNA library from a single-cell quantity of mRNA without PCR amplification. *Nucleic Acids Res* **36**, e92 (2008).
5. Zuker, M. Mfold web server for nucleic acid folding and hybridization prediction. *Nucleic Acids Res* **31**, 3406–3415 (2003).
6. Tabata, H. & Nakajima, K. Labeling embryonic mouse central nervous system cells by in utero electroporation. *Dev Growth Differ* **50**, 507–511 (2008).
7. Shaner, N. C. *et al.* Improved monomeric red, orange and yellow fluorescent proteins derived from Discosoma sp. red fluorescent protein. *Nat Biotechnol* **22**, 1567–1572 (2004).
8. Lein, E. S. *et al.* Genome-wide atlas of gene expression in the adult mouse brain. *Nature* **445**, 168–176 (2007).
9. Guzowski, J. F., McNaughton, B. L., Barnes, C. A. & Worley, P. F. Environment-specific expression of the immediate-early gene Arc in hippocampal neuronal ensembles. *Nat Neurosci* **2**, 1120–1124 (1999).
10. Kobayashi, K. *et al.* One-step RT-PCR without initial RNA isolation sStep for laser-microdissected tissue sample. *J Vet Med Sci* **65**, 917–919 (2003).
11. Burbach, G. J., Dehn, D., Del Turco, D. & Deller, T. Quantification of layer-specific gene expression in the hippocampus: effective use of laser microdissection in combination with quantitative RT-PCR. *J Neurosci Methods* **131**, 83–91 (2003).
12. Sonne, S. B. *et al.* Optimizing staining protocols for laser microdissection of specific cell types from the testis including carcinoma in situ. *PLoS One* **4**, e5536 (2009).
13. Tabata, H. & Nakajima, K. Efficient in utero gene transfer system to the developing mouse brain using electroporation: visualization of neuronal migration in the developing cortex. *Neuroscience* **103**, 865–872 (2001).
14. Eppig, J. T. & Strivens, M. Finding a mouse: the International Mouse Strain Resource (IMSR). *Trends Genet* **15**, 81–82 (1999).
15. Shinohara, Y. *et al.* Hippocampal CA3 and CA2 have distinct bilateral innervation patterns to CA1 in rodents. *Eur J Neurosci* **35**, 702–710 (2012).
16. Ramirez-Amaya, V. *et al.* Spatial exploration-induced Arc mRNA and protein expression: evidence for selective, network-specific reactivation. *J Neurosci* **25**, 1761–1768 (2005).
17. Guzowski, J. F., Setlow, B., Wagner, E. K. & McGaugh, J. L. Experience-dependent gene expression in the rat hippocampus after spatial learning: a comparison of the immediate-early genes Arc, c-fos, and zif268. *J Neurosci* **21**, 5089–5098 (2001).
18. Sarantis, K., Antoniou, K., Matsokis, N. & Angelatou, F. Exposure to novel environment is characterized by an interaction of D1/NMDA receptors underlined by phosphorylation of the NMDA and AMPA receptor subunits and activation of ERK1/2 signaling, leading to epigenetic changes and gene expression in rat hippocampus. *Neurochem Int* **60**, 55–67 (2012).
19. Herdegen, T. & Leah, J. D. Inducible and constitutive transcription factors in the mammalian nervous system: control of gene expression by Jun, Fos and Krox, and CREB/ATF proteins. *Brain Res Brain Res Rev* **28**, 370–490 (1998).
20. Cheval, H. *et al.* Distinctive features of Egr transcription factor regulation and DNA binding activity in CA1 of the hippocampus in synaptic plasticity and consolidation and reconsolidation of fear memory. *Hippocampus* **22**, 631–642 (2012).
21. Schwartz, N., Schohl, A. & Ruthazer, E. S. Activity-dependent transcription of BDNF enhances visual acuity during development. *Neuron* **70**, 455–467 (2011).
22. Zumbrun, S. D., Hoffman, B. & Liebermann, D. A. Distinct mechanisms are utilized to induce stress sensor gadd45b by different stress stimuli. *J Cell Biochem* **108**, 1220–1231 (2009).
23. Okuno, H. *et al.* Inverse synaptic tagging of inactive synapses via dynamic interaction of Arc/Arg3.1 with CaMKIIbeta. *Cell* **149**, 886–898 (2012).
24. Klaus, A., Yu, S. & Plenz, D. Statistical analyses support power law distributions found in neuronal avalanches. *PLoS One* **6**, e19779 (2011).
25. Ueda, H. R. *et al.* Universality and flexibility in gene expression from bacteria to human. *Proc Natl Acad Sci U S A* **101**, 3765–3769 (2004).
26. Rozen, S. & Skaletsky, H. Primer3 on the WWW for general users and for biologist programmers. *Methods Mol Biol* **132**, 365–386 (2000).

Acknowledgements

This work was supported by the research project of the Cooperative Research of Leica-Microsystems and the University of Tokyo to M.K., and the Strategic Research Program for Brain Sciences (SRPBS) of the Ministry of Education, Culture, Sports, Science and Technology to C.T., Grant-in-Aid to M.K. and C.T. from the Japan Society for the Promotion of Science. R.N. is an employee of Leica Microsystems. We thank Dr. K. Nakajima of Keio University for his kind guidance concerning the *in utero* electroporation technique, Drs. S. Shibata of Waseda University and C. Watanabe of the University of Tokyo, K. Tani and Y. Takahashi of Tokyo University of Pharmacy and Life Sciences for their helpful discussions, and A. Shimazaki and Y. Hirasawa for their excellent technical assistance.

Author contributions

M.K., W.Y., R.N. and C.T. designed experiments. W.Y. established the method to determine ultra-microquantities of RNA. W.Y., N.E., A.K., A.H., T.E. and T.S. performed experiments. C.T., W.Y. and M.K. wrote the paper.

Additional information

Supplementary information accompanies this paper at http://www.nature.com/scientificreports

Competing financial interests W.Y., N.E., A.K., A.H., T.E., T.S., M.K. and C.T. declare no competing financial interests. R.N. is an employee of Leica Microsystems K.K.

How to cite this article: Yoshioka, W. *et al.* Fluorescence laser microdissection reveals a distinct pattern of gene activation in mouse hippocampal regions. *Sci. Rep.* **2**, 783; DOI:10.1038/srep00783 (2012).